Two-Dimensional Streptavidin Crystals on Giant Lipid Bilayer Vesicles

Pasut Ratanabanangkoon,[†] Michael Gropper,[‡] Rudolf Merkel,[§] Erich Sackmann,[‡] and Alice P. Gast*

Department of Chemical Engineering, Stanford University, Stanford, California 94305-5025, Department of Biophysics E22, Technical University of Munich, D-85748 Garching, Germany, Forschungszentrum Jülich, Institut für Schichten und Grenzflächen (ISG-4), D-52425 Jülich, Germany, and Department of Chemical Engineering, Massachusetts Institute of Technology, Cambridge, Massachusetts, 02139

Received January 22, 2002. In Final Form: March 27, 2002

Streptavidin was crystallized on giant bilayer vesicles (20−60 μm) in sucrose solution at various pH values. The streptavidin-coated vesicles exhibited unique roughened spherical and prolate ellipsoidal shapes, illustrating resistance to curvature of the two-dimensional crystals. Studies indicated that the spheroids and prolate ellipsoids correspond to different crystal morphologies. Through confocal microscopy, the various crystal morphologies on vesicle surfaces were observed under different solution conditions. Unlike two-dimensional (2D) streptavidin crystals grown in ionic buffer that assume the *P*1, *P*2, and *C*222 lattices at pH 4, 5.5, and 7, respectively (Wang et al. *Langmuir* **1999**, *15*, 1541), crystals grown in sucrose with no added salt show only the lowest density *C*222 lattice due to strong electrostatic interactions.

Introduction

The delicate balance of forces governing ordering in complex fluids produces many interesting and useful phenomena.[1] Ordering processes of particular interest are those occurring in the two-dimensional assemblies of lipids and proteins that create cell walls. These include interesting structural changes occurring in the two-dimensional protein coat on the tail sheath of the bacteriophage injection apparatus during its penetration into a bacterium[2] and the S-layer proteins coating bacterial cell surfaces.[3] We believe that the complex phenomena occurring in these biological systems can be traced to simple intermolecular interactions triggered by changes in pH, ionic strength, or polarity of the fluid environment. It is our goal to unravel these biological mysteries through systematic experiments on simple systems.

The protein streptavidin has been widely studied due to its unique properties and potential uses.[4−7] The ability for streptavidin to crystallize into well-ordered arrays creates potential for numerous applications in the field of biosensors and biomaterials.[8−10] The fact that streptavidin molecules contain four biotin binding sites, two pairs on opposite side of the molecules,[6] makes them ideal as strong cross-linkers. Due to the unusually high binding affinity for biotin (10^{-15} M),[5] the streptavidin−biotin system has been widely exploited for various physical and biological applications.[4,11−14] Two-dimensional (2D) crystallization of streptavidin has been studied on various surfaces such as lipid monolayers at the air−water interface,[15−19] lipid bilayer membranes at solid−liquid interfaces,[20] and lipid nanotubes.[21,22] Streptavidin had also been attached to nanometer-size liposomes[13,23] for linking to other biomolecules, but to our knowledge, the study of streptavidin crystallization on liposomes has not been reported.

In this work, we have crystallized streptavidin on the surfaces of giant (>10 μm) lipid bilayer vesicles. Giant unilamellar vesicles,[24] typically ranging from 10 to 100

* To whom correspondence should be addressed at Massachusetts Institute of Technology: phone (617) 253-1403; fax (617) 253-8388; e-mail gast@mit.edu.
[†] Stanford University; e-mail pasut@leland.stanford.edu.
[‡] Technical University of Munich; e-mail michael.gropper@web.de or sackmann@physik.tu-muenchen.de.
[§] Institut für Schichten und Grenzflächen; e-mail r.merkel@fz-juelich.de.

(1) Gast, A. P.; Russel, W. B. *Phys. Today* **1998**, *51*, 24−30.
(2) Olson, G. B.; Hartman, H. *J. Phys.* **1982**, *43*, 855−865.
(3) Sleytr, U. B.; Sara, M.; Messner, P.; Pum, D. *J. Cell. Biochem.* **1994**, *56*, 171−176.
(4) Bayer, E. A.; Wilcheck, M. *Avidin−biotin technology*; Academic Press: San Diego, CA, 1990; Vol. 184.
(5) Bayer, E. A.; Benhur, H.; Wilchek, M. *Methods Enzymol.* **1990**, *184*, 80−89.
(6) Weber, P. C.; Ohlendorf, D. H.; Wendoloski, J. J.; Salemme, F. R. *Science* **1989**, *243*, 85−88.
(7) Green, N. M. *Methods Enzymol.* **1990**, *184*, 51−67.
(8) Samuelson, L. A.; Wiley: B.; Kaplan, D. L.; Sengupta, S.; Kamath, M.; Lim, J. O.; Cazeca, M.; Kumar, J.; Marx, K. A.; Tripathy, S. K. *J. Intell. Mater. Syst. Struct.* **1994**, *5*, 305−310.
(9) McLean, M. A.; Stayton, P. S.; Sligar, S. G. *Anal. Chem.* **1993**, *65*, 2676−2678.
(10) Koppenol, S.; Stayton, P. S. *J. Pharm. Sci.* **1997**, *86*, 1204−1209.
(11) Furst, E. M.; Gast, A. P. *Phys. Rev. Lett.* **1999**, *82*, 4130−4133.
(12) Bayer, E. A.; Wilchek, M. *J. Chromatogr.* **1990**, *510*, 3−11.
(13) Müller, W.; Ringsdorf, H.; Rump, E.; Wildburg, G.; Zhang, X.; Angermaier, L.; Knoll, W.; Liley, M.; Spinke, J. *Science* **1993**, *262*, 1706−1708.
(14) Perkins, T. T.; Quake, S. R.; Smith, D. E.; Chu, S. *Science* **1994**, *264*, 822−826.
(15) Scheuring, S.; Müller, D. J.; Ringler, P.; Heymann, J. B.; Engel, A. *J. Microsc.* **1999**, *193*, 28−35.
(16) Darst, S. A.; Ahlers, M.; Meller, P. H.; Kubalek, E. W.; Blankenburg, R.; Ribi, H. O.; Ringsdorf, H.; Kornberg, R. D. *Biophys. J.* **1991**, *59*, 387−396.
(17) Ku, A. C.; Darst, S. A.; Kornberg, R. D.; Robertson, C. R.; Gast, A. P. *Langmuir* **1992**, *8*, 2357−2360.
(18) Hemming, S. A.; Bochkarev, A.; Darst, S. A.; Kornberg, R. D.; Ala, P.; Yang, D. S. C.; Edwards, A. M. *J. Mol. Biol.* **1995**, *246*, 308−316.
(19) Frey, W.; Schief, W. R.; Pack, D. W.; Chen, C. T.; Chilkoti, A.; Stayton, P.; Vogel, V.; Arnold, F. H. *Proc. Natl. Acad. Sci. U.S.A.* **1996**, *93*, 4937−4941.
(20) Calvert, T. L.; Leckband, D. *Langmuir* **1997**, *13*, 6737−6745.
(21) Ringler, P.; Müller, W.; Ringsdorf, H.; Brisson, A. *Chem. Eur. J.* **1997**, *3*, 620−625.
(22) Wilson-Kubalek, E. M.; Brown, R. E.; Celia, H.; Milligan, R. A. *Proc. Natl. Acad. Sci. U.S.A.* **1998**, *95*, 8040−8045.
(23) Velev, O. D. *Adv. Biophys.* **1997**, *34*, 139−157.
(24) Luisi, P. L.; Walde, P. *Giant Vesicles*; John Wiley & Sons: Ltd: New York, 2000; Vol. 6.

10.1021/la025568v CCC: $22.00
Published on Web 05/03/2002

μm in size, can be prepared through gentle hydration,[25,26] rapid evaporation,[27] or electroformation[28−30] methods. With a size comparable to biological cells, they can be easily studied and manipulated and have led to significant understanding of cell membrane properties such as membrane adhesion,[31,32] budding,[33,34] and deformation.[35] Our goal in this study is to understand the interplay between protein layer crystallinity, vesicle morphology, and the crystallization process. We have observed that streptavidin crystals grown on lipid monolayers at the air−water interface have pH-dependent morphologies. Concurrent addition of the homologous protein avidin allows the development of unique crystal shapes ranging from needlelike to chiral inverse S-shaped and X-shaped crystals, corresponding to different crystal structures.[36] Avidin does not crystallize due to heterogeneous oligosaccharide chains resulting from glycosylation and has been added as a noncrystallizable impurity in 2D streptavidin crystallization to dilute the streptavidin concentration at the surface and to allow uninhibited growth of large crystal domains.[17,36−38] Whether these structures will persist when grown on a vesicle surface in sucrose solutions of lower ionic strength is the first question. Further investigating the crystallization processes on vesicles allows us to deduce the influence of a surface crystalline layer on vesicle shape. Giant vesicles are ideal for this investigation due to their large surface area, moderate curvature, and high flexibility.

This study may also lead to applications in biotechnology through the creation of well-ordered arrays of biological linkers on a large spherical support, suitable for efficient immobilization of various functionalized enzyme and affinity ligands. Although similar concepts have been reported with s-layer coated nanometer-sized liposomes,[39] immobilization of other functionalized molecules onto s-layers requires activation of the protein carboxylate groups through the use of carbodiimide. Once activated, the groups are subject to rapid hydrolysis, thus reducing the coupling efficiency over time and frequently resulting in significant number of defects and holes in the new macromolecular layer. With the streptavidin−biotin system, no such activation is necessary, and the coupling affinity for biotinylated molecules remains high. In conjunction with the fact that streptavidin is widely commercially available and less expensive compared to s-layers, crystalline streptavidin layers should provide an effective template for immobilizing macromolecules when a high degree of order and coupling efficiency is desired.

Material and Methods

Vesicle Electroformation. Giant SOPC vesicles were made via electroformation[30] between two ITO (indium tin oxide) coated glass (5 cm × 4.5 cm × 0.1 cm) electrodes in a Teflon chamber. The chamber consists of a block of Teflon with a slot sufficiently large to submerge the two electrodes in the formation medium with a 0.5 mm gap in between. Before use, the Teflon chamber and electrodes are thoroughly cleaned by repeated bath sonication and rinsed with copious amounts of Milli-Q water (Millipore, Bedford, MA). The lipid solution consisted of a 1 mg/mL mixture of 10 wt % biotin-X-DHPE (*N*-[6-(biotinoylamino)hexanoyl]-1,2-dihexadecanoyl-*sn*-glycero-3-phosphoethanolamine, triethylammonium salt) (Molecular Probes, Eugene, OR) and SOPC (1-stearoyl-2-oleoyl-*sn*-glycero-3-phosphocholine) (Avanti, Alabaster, AL) in pure chloroform. An aliquot of about 40 μL was spread into a thin film on each ITO electrode and left to dry overnight in a vacuum chamber. The two lipid-coated electrodes were then put together in the Teflon chamber filled with 608 mOsm sucrose solution. A Teflon spacer between the two glass surfaces prevents contact. The vesicles were formed in an AC electric field (1 V, 10 Hz) for approximately 2 h at room temperature.

A small aliquot of the stock vesicle solution was injected into a viewing cell filled with equal or slightly higher osmolality glucose solution and 1 mg/mL bovine serum albumin (BSA) (Sigma, St. Louis, MO) to prevent the vesicles from adhering to the glass surface. The difference in solution density causes the vesicles to sink to the bottom for easy observation, while the index of refraction difference enhances contrast when viewed by differential interference contrast (DIC). DIC microscopy was performed with an inverse microscope (Axiovert 100S TV, Carl Zeiss, Jena, Germany) equipped with an LD-Achroplan 40 × 0.60 Korr lens (Carl Zeiss) and the recommended accessories for DIC.

The vesicles were mostly between 20 and 60 micrometers in diameter and remained stable in unbuffered sucrose solution for at least 12 h. In these experiments, the vesicles were used within 5 h after electroformation.

Protein Labeling. Streptavidin and avidin were purchased from Prozyme (San Leandro, CA). A portion of the two proteins was labeled with Texas Red succinimidyl ester (single isomer) (Molecular Probes, Eugene, OR) according to the supplied protocol with minor modifications. Briefly, the proteins were dissolved in 100 mM sodium bicarbonate buffer, pH 8.3, to a concentration of 2 mg/mL. The fluorescent dye was then dissolved in reagent-grade dimethyl sulfoxide (DMSO; Sigma, St. Louis, MO) to a concentration of 10 mg/mL and added to the protein solution at a ratio of 1 dye/5 streptavidin molecules. The mixture was stirred in the dark at room temperature for 2 h. The labeled protein was separated from the unreacted dye by passage through a size-exclusion column packed with Sephadex G25 (Sigma, St. Louis, MO) and eluted with 50 mM sodium phosphate, pH 7.0. The Texas Red dye was chosen because of its high resistance to photobleaching. The final protein concentration and degree of labeling were determined on a spectrophotometer by measuring the absorbance at 280 and 595 nm, respectively. The final degree of labeling was approximately 1 dye/10 streptavidin molecules.

Another portion of the remaining streptavidin and avidin was labeled with FITC (fluorescein isothiocyanate) at a ratio of 2 dyes/protein molecule according to the method described by Nargessi and Smith.[40] The FITC-labeled proteins were used to grow 2D streptavidin crystals on lipid monolayers.

We have observed that labeling streptavidin with fluorescent dyes at these levels does not change the morphologies or structures of crystals grown on lipid monolayers at the air−water interface and that they were the same as those obtained with unlabeled streptavidin.[38]

Crystal Formation on Vesicle Surfaces. To grow streptavidin crystals on the surface of SOPC/biotin-X-DHPE vesicles,

(25) Reeves, J. P.; Dowben, R. M. *J. Cell Physiol.* **1969**, *73*, 49−60.
(26) Needham, D.; Evans, E. *Biochemistry* **1988**, *27*, 8261−8269.
(27) Moscho, A.; Orwar, O.; Chie, D. T.; Modi, B. P.; Zare, R. N. *Proc. Natl. Acad. Sci. U.S.A.* **1996**, *93*, 11443−11447.
(28) Bagatolli, L. A.; Parasassi, T.; Gratton, E. *Chem. Phys. Lipids* **2000**, *105*, 135−147.
(29) Angelova, M.; Dimitrov, D. S. *Prog. Colloid Polym. Sci.* **1988**, *76*, 59−67.
(30) Angelova, M. I.; Dimitrov, D. S. *Faraday Discuss. Chem. Soc.* **1986**, *81*, 303−311.
(31) Evans, E.; Metcalfe, M. *Biophys. J.* **1984**, *45*, 715−720.
(32) Maier, C. W.; Behrisch, A.; Kloboucek, A.; Simson, D. A.; Merkel, R. *Eur. Phys. J. E* **2001**, *6*, 273−276.
(33) Dobereiner, H. G.; Kas, J.; Noppl, D.; Sprenger, I.; Sackmann, E. *Biophys. J.* **1993**, *65*, 1396−1403.
(34) Sackmann, E. *FEBS Lett.* **1994**, *346*, 3−16.
(35) Evans, E. A.; Skalak, R. *Mechanics and Thermodynamics of Biomembranes*; CRC Press: Boca Raton, FL, 1980.
(36) Wang, S. W.; Robertson, C. R.; Gast, A. P. *Langmuir* **1999**, *15*, 1541−1548.
(37) Farah, S. J.; Wang, S. W.; Chang, W. H.; Robertson, C. R.; Gast, A. P. *Langmuir* **2001**, *17*, 5731−5735.
(38) Wang, S. W.; Poglitsch, C. L.; Yatcilla, M. T.; Robertson, C. R.; Gast, A. P. *Langmuir* **1997**, *13*, 5794−5798.
(39) Küpcü, S.; Sára, M.; Sleytr, U. B. *Biochim. Biophys. Acta* **1995**, *1235*, 263−269.
(40) Nargessi, R. D.; Smith, D. S. *Methods Enzymol.* **1986**, *122*, 67−72.

we added 80 μL of the newly electroformed vesicles to 420 μL of the protein solution. The protein solution consists of either pure streptavidin, streptavidin/TR avidin mixture, TR streptavidin/avidin mixture, or pure TR streptavidin in 608 mOsm sucrose at an overall concentration of 10−30 μg/mL. At 25 °C, the saturation limit of sucrose in water is approximately 2160 mOsm (1.97 M).[41] Although not required for crystallization, high concentrations of sucrose showed slight buffering capacity and assisted in the precise control of the solution pH. Pure 608 mOsm sucrose solution has a pH of approximately 5.0, and a pH range from 4 to 7.5 of the protein solution was controlled by adding 0.1−2 μL of either 500 mM Tris, pH 10, or 500 mM MES, pH 3.15. MES and Tris were chosen since they provide greater stability to the vesicles than other types of buffers tested. The buffers were added mainly to adjust the pH of the solution, despite the suboptimal buffering capacity under our particular experimental pH conditions. Care was taken to keep the total buffer concentration in the protein solution under 2 mM, as higher buffer concentrations greatly reduce the stability of the vesicles. The vesicles were incubated in the protein solution for at least 3 h at room temperature before observation.

Confocal Microscopy. We transferred the protein-coated vesicles to a viewing cell filled with 618 mOsm glucose solution containing 1 mg/mL BSA. The lower density of surrounding glucose solution causes the sucrose-filled vesicles to sink to the bottom of the cell and remain still during observation.

The confocal laser scanning microscope consists of a scanning unit (Noran, Middleton, WI) attached to a Zeiss Axiovert 100 TV (Zeiss, Germany). Texas Red molecules on the vesicles were excited with a laser passing through a 568/590LP excitation/emission filter set and viewed with an LD-Achroplan 40 × 0.60 Korr lens objective (Carl Zeiss). To prevent image superimposition of crystals from opposite sides of the vesicle, we took image slices of only the upper half of the vesicles at 0.5−1 μm intervals and created a three-dimensional reconstruction with the Intervision software package provided by Noran on a Silicon Graphics Indy II computer (SGI Inc., Mountain View, CA).

Crystal Formation on Lipid Monolayer. We followed the procedures for 2D crystallization of streptavidin at the air−water interface described by Wang et al.[38] with some modifications. Briefly, eight circular wells (19 mm diameter, 3.5 mm deep) were made on a 10 cm × 8 cm × 0.6 cm piece of black Delrin (Dupont, Wilmington, DE). We drilled a small, needle-size injection port into the side of each well so that material could be injected into the solution without disrupting the surface. This design allowed us to perform eight crystallization experiments simultaneously. Before each use, the wells were soaked in chloroform for 1 h, rinsed with chloroform, and rinsed with copious amount of filtered Milli-Q water. The subphase consisted of either pH-adjusted 608 mOsm sucrose solution or a sodium phosphate buffer containing 50 mM NaH_2PO_4 and 500 mM NaCl, pH 4−7. We spread a predetermined amount of 0.15 mg/mL 10:1 (wt %) mixture of SOPC and biotin-X DHPE in 2:1 chloroform/methanol onto the surface to achieve a surface pressure of 25−35 mN/m. The solvent was allowed to evaporate for 15 min before a small aliquot of either TR streptavidin or streptavidin/TR avidin mixture was injected into the subphase through the injection port to a final concentration of 20 μg/mL. The wells were left in the dark in a covered, hydrated environment for at least 6 h before observation in situ via fluorescence microscopy with the 20×/0.50 NA Zeiss Plan-Neofluar objective on a Zeiss Axioplan microscope (Zeiss, Germany) equipped with a mercury arc lamp and 530−585/600/615 nm excitation/dichroic beam splitter/emission filter set. Images were taken with a Hamamatsu ORCA cooled CCD digital camera (Hamamatsu, Japan) controlled by SimplePCI imaging software (Compix, Inc., Cranberry Township, PA).

To prepare the samples for transmission electron microscopy (TEM), the crystals were first stabilized by cross-linking with 50% glutaraldehyde for 4 h. This process does not alter the crystal structure to within our resolution.[38] The crystals were transferred onto carbon-coated copper grids (Ted Pella Inc., Redding, CA), washed, and stained with 1% uranyl acetate for 1 min. Details of the transfer procedure can be found in Wang et al.[36]

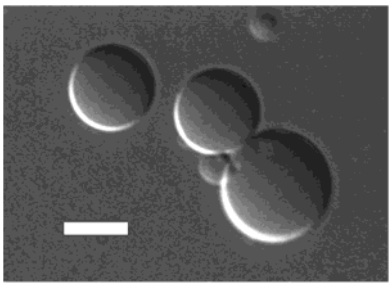

Figure 1. DIC microscopic image of bare SOPC/biotin-X-DHPE vesicles. Scale bar is 10 μm.

The TEM images were taken on a Phillips CM20 electron microscope at 42000−55000× and the negatives were digitized by use of a Leaf45 scanner (Leaf Systems, Inc., Southborough, MA), and processed by CRISP crystallographic image processing software[42] (Sollentuna, Sweden).

Results and Discussion

Figure 1 shows a differential interference contrast (DIC) image of bare SOPC/biotin-X-DHPE vesicles. The vesicles were perfectly spherical and elastic, similar to those made of pure SOPC. When placed in a hypertonic glucose solution, the vesicles shrink and thermal fluctuations are clearly seen on the membrane.

When the bare vesicles were incubated in 100% avidin solution, they became more rigid and membrane fluctuations were no longer seen in hypertonic solution. The vesicles remained smooth and spherical and showed an elastic recovery after deformation similar to that of bare vesicles.[43]

Confocal Study of Streptavidin Crystals on Vesicle Surfaces. Vesicles incubated with a mixture of streptavidin and TR avidin showed large streptavidin crystallites when viewed under fluorescence. The number and size of the crystallites increased with the streptavidin:TR avidin ratio. Most vesicles coated with the streptavidin/avidin mixture remained spherical, although at high streptavidin ratios, some distortions were observed. In Figure 2 we show three-dimensional (3D) reconstructed confocal microscopic images of the protein-coated vesicles grown in sucrose at pH values ranging from 4.3 to 7. The crystals of unlabeled streptavidin appear as black domains surrounded by white regions of fluorescent avidin.

A number of observations can be made from Figure 2. Crystals tend to form more readily in sucrose at pH 5.2 or below. At pH 6.3, only thin, elongated needles form, while no macroscopic crystals were seen on the vesicles at pH 7 or above. This transition from abundant to no crystallization coincides well with the observed isoelectric point (p*I*) of 5−6 for streptavidin.[7] Unlike crystals grown in ionic buffer solutions (50 mM NaH_2PO_4 and 500 mM NaCl) at the air−water interface,[36] the crystals in Figure 2 do not follow a definite morphological trend. Despite the lack of a trend, the X-shaped and H-shaped crystallites closely resemble those having *C*222 symmetry found on monolayers. The crystallites also showed the preferential growth direction characteristic of anisotropic conformational changes in the streptavidin molecules upon biotin binding.[6] We will later show that crystals grown on monolayers over the same sucrose solution show the same *C*222 symmetry, in agreement with the morphological observations.

(41) Mathlouthi, M.; Reiser, P. *Sucrose: Properties and applications*; Blackie Academic & Professional: London and New York, 1995.

(42) Hovmoller, S. *Ultramicroscopy* **1992**, *41*, 121−135.

(43) Ratanabanangkoon, P.; Gropper, M.; Merkel, R.; Sackmann, E.; Gast, A. P. Manuscript in preparation.

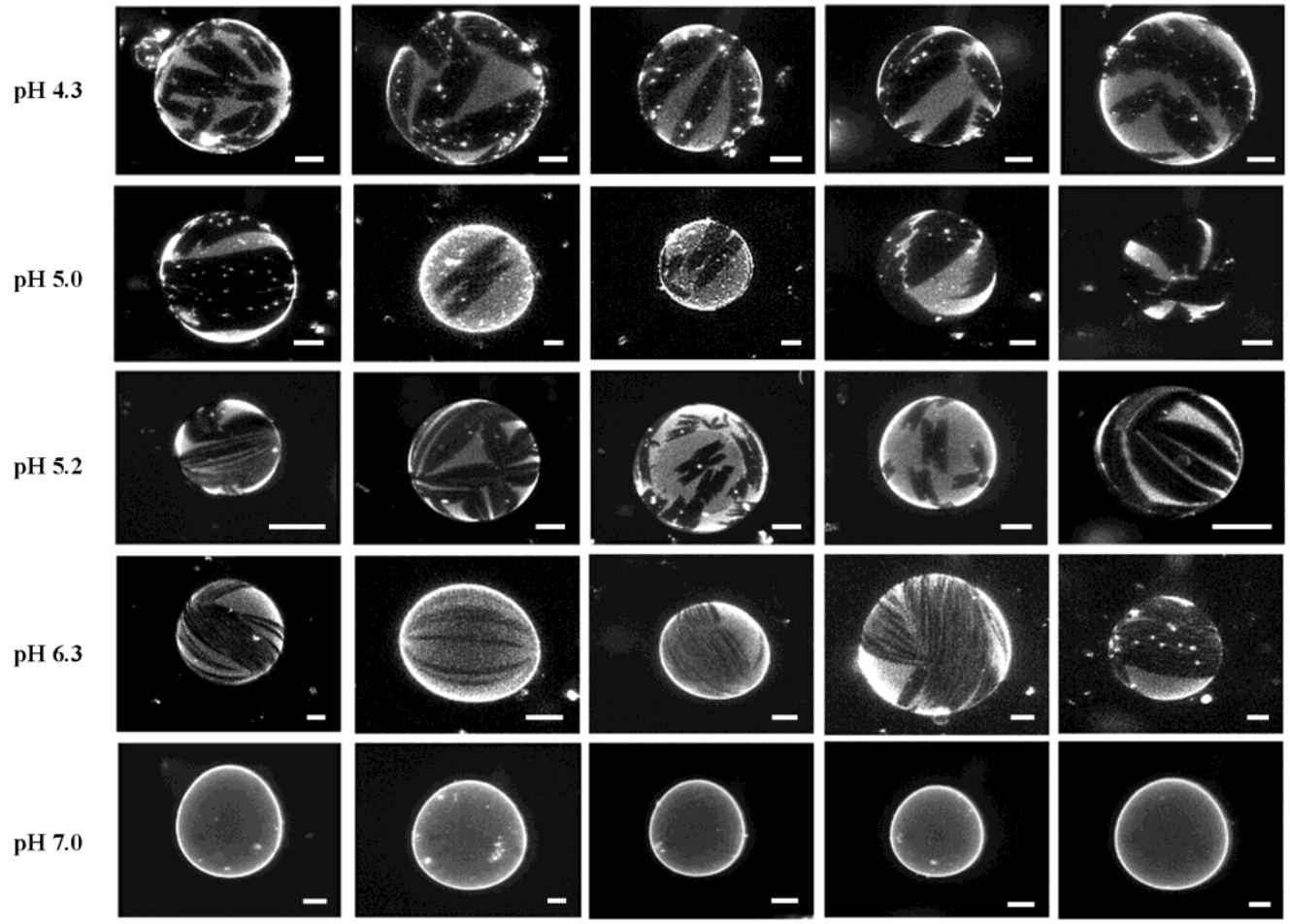

Figure 2. Three-dimensional reconstructed confocal microscopic images of various streptavidin crystal morphologies on giant bilayer vesicles at the indicated pH. The vesicles were coated with a 1:1 mixture of streptavidin and Texas Red avidin. To prevent crystal domains from opposite sides of the vesicles from superimposing, image slices (1 μm thickness) of only the upper half of each vesicle were taken and digitally reconstructed. Streptavidin crystals appear black surrounded by noncrystallizable Texas Red avidin (white). Note that at pH 7 no streptavidin crystals can be seen. Scale bar under each vesicle represents 10 μm.

Vesicle Shapes with Streptavidin Crystals. Vesicles coated with 100% streptavidin were very different from the bare and avidin-coated vesicles. Instead of having smooth spherical surfaces, the vesicles became rigid and distorted with the presence of numerous creases and facets indicative of a rigidification due to crystal formation. As with vesicles coated with 100% avidin and streptavidin/avidin mixtures, thermal undulations were not visible. We observe two typical vesicle morphologies shown in Figure 3. The first type (Figure 3A) is spherical vesicles with rough surfaces, while Figure 3B shows a prolate ellipsoidal vesicle with a relatively smoother surface. According to micropipet studies, both types of vesicles are very rigid and exhibit plastic behavior, as indicated by permanent deformations when they are stressed beyond their yield point.[43]

The ellipsoidal vesicles also contained unique ridges on the surface running along the major axis. These two morphologies were typically seen coexisting within the same sample with an increasing number of ellipsoids at higher pH.

Table 1 summarizes the effect of incubation time and incubation solution pH on the relative number of the two different vesicle morphologies. The bare vesicles were incubated in 608 mOsm sucrose solution containing 20 μg/mL streptavidin at either pH 5 or pH 6. After the specified incubation times, a small aliquot was taken and inspected in 660 mOsm glucose solution. Fewer than half

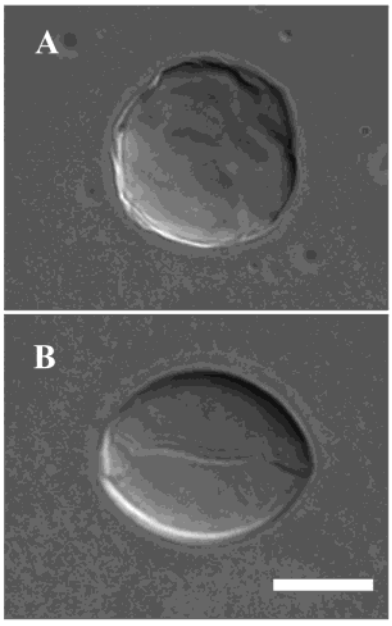

Figure 3. DIC microscopic images show two shapes observed among streptavidin-coated vesicles. (A) Rough surfaces have many ridges and edges. (B) Ellipsoids are smoother with characteristic ridges running parallel to the major axis. Scale bar is 20 μm.

Table 1. Effect of Incubation Time and Incubation Solution pH on Vesicle Morphologies

	pH 5			pH 6		
incubation time (h)	% ellipsoids	% spheres	n	% ellipsoids	% spheres	n
1	36	64	134	43	57	112
3	34	66	126	60	40	132
5	36	64	131	65	35	133

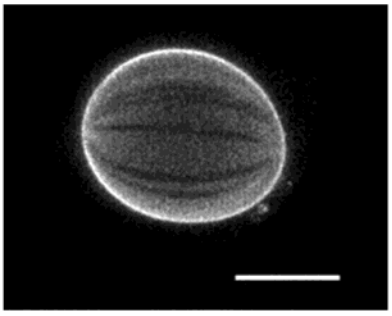

Figure 4. Three-dimensional reconstructed confocal microscopic image of a prolate ellipsoid vesicle coated with a mixture of Texas Red avidin and streptavidin. The streptavidin crystals can be seen as thin, dark longitudinal lines. Scale bar is 20 μm.

of the vesicles incubated in pH 5 sucrose solution transformed into prolate ellipsoids, while the majority of vesicles incubated at pH 6 made such a transformation. It is also noticed that most of the morphological changes occurred within 1 h when vesicles were incubated in the pH 5 sucrose solution. On the other hand, vesicles incubated at pH 6 showed a much slower transition over a period of at least 3 h.

The presence of prolate ellipsoidal vesicles was almost exclusively seen in vesicles coated with 100% streptavidin. Vesicles usually remain spherical in the presence of noncrystallizable avidin. One of the exceptions, an ellipsoidal vesicle coated with a streptavidin/avidin mixture, is shown in Figure 4. Unlike most streptavidin/avidin-coated vesicles, where the streptavidin crystallites form isolated and randomly oriented domains, the vesicle in Figure 4 shows long, continuous crystals across the entire vesicle. The formation of a thin, elongated shape of the streptavidin crystals on the vesicle suggests a strong preferred growth direction, as seen with streptavidin crystals grown on lipid monolayers.[36]

The confocal microscopy suggested that the ellipsoids were composed of thin, continuous, needle-shaped crystals with parallel growth directions. The strong crystal shape anisotropy along with the parallel growth pattern resulted in the elongation of the vesicle along one direction, as the bending rigidity of the crystallites is higher than that of the surrounding matrix. At high pH, fewer nucleation sites were present due to retardation factors such as electrostatic repulsion, and crystal growth was relatively slower than that at lower pH. The slow crystal growth and fewer nucleation sites allowed the formation of large crystallites with fewer defects, hence the smoother surface compared to the roughened spherical vesicles.

The distortion of vesicles due to crystallized protein molecules at the surface has been observed with bacterium *Comamonas acidovorans* surface layer proteins when reconstituted on lipid vesicles.[44] Micrometer-size vesicles covered with protein crystals were distorted into various shapes such as spheres, cylinders, and cones. The protein is thought to anchor into the membrane via a small hydrophobic domain. Through electron microscopy, Paul and co-workers[44] have shown that distortion of the vesicle surface requires the proteins to form 2D self-contained and continuous crystalline envelopes around parts of the surface. This is analogous to our system. The strong coupling between streptavidin and the lipid membrane was provided via the streptavidin−biotin interaction with the biotinylated lipid acted as hydrophobic anchors securing the proteins to the vesicle surface. Although the interaction between streptavidin and biotin is very strong, the system can relax due to reorientation and relocation of the streptavidin−biotinylated lipid complex within the fluid matrix. The 2D crystals observed here (space group *C*222) have been shown to be sufficiently flat to template the growth of 3D (space group $I_1$22) streptavidin crystals, which consist of a stack of the 2D array.[18] This shows that the *C*222 form of 2D streptavidin crystal is capable of forming flat crystal domains and should not impose any significant bending on the vesicle membrane. The presence of multiple flat crystalline domains separated by defects and grain boundaries results in the rough vesicle surface observed. Both effects, relaxation within the fluid matrix and flatness of the crystals, are important for the integrity of the giant unilamellar vesicles during crystal growth. The observed continuous, self-contained crystal envelope also agrees with our observation that ellipsoidal vesicles have smoother surfaces, indicating the presence of larger crystals with fewer defects.

Crystals on the roughened spheres grew differently from those of ellipsoids. The roughened spheres tend to be found more often below pH $\sim$ 5.5. We observed from monolayer experiments that nucleation occurs much faster at lower pH; the same trend was observed on bilayer vesicles yielding more but smaller crystallites on the surface. [This applies to vesicles coated with 100% streptavidin. In vesicles that are coated with streptavidin/avidin mixtures such as those shown in Figure 2, the presence of non-crystallizable avidin dilutes the streptavidin concentration at the vesicle surface. This results in slower crystal growth and larger domains as seen on some of the vesicles.] Due to the rapid nucleation and growth of the crystallites, they tend to be randomly oriented, creating many defects and grain boundaries. As a result, the crystallites are not sufficiently aligned to impose a uniform curvature on the entire vesicle. Thus, these vesicles remain relatively round with patches of small rigid crystallites on the surface.

As mentioned previously, the crystals observed on bilayer vesicles lack a clear morphological trend at different pH values unlike those grown in ionic buffer solutions. Thus, the crystal structure could not be readily deduced from morphology and previous experiences with monolayer systems.

Monolayer Experiments. The obvious question remains: do streptavidin crystals grown on bilayer vesicles in sucrose exhibit the same diverse crystal structures at various pH values as those grown in buffer systems on lipid monolayers? Because the SOPC/biotin-X-DHPE vesicles were not stable in high ionic strength solutions, we could not grow streptavidin crystals on vesicles in the buffer normally used in monolayer experiments. It is thus not possible to compare crystal morphologies from the two systems in buffer.

Instead, we address this question through a series of monolayer experiments. We grew streptavidin crystals on a lipid monolayer with sucrose solution as a subphase at various pH values. Figure 5 shows a comparison of crystal morphologies at different pH values.

In sucrose, streptavidin crystals were denser and more abundant when grown with 100% streptavidin. The

(44) Paul, A.; Engelhardt, H.; Jakubowski, U.; Baumeister, W. *Biophys. J.* **1992**, *61*, 172−188.

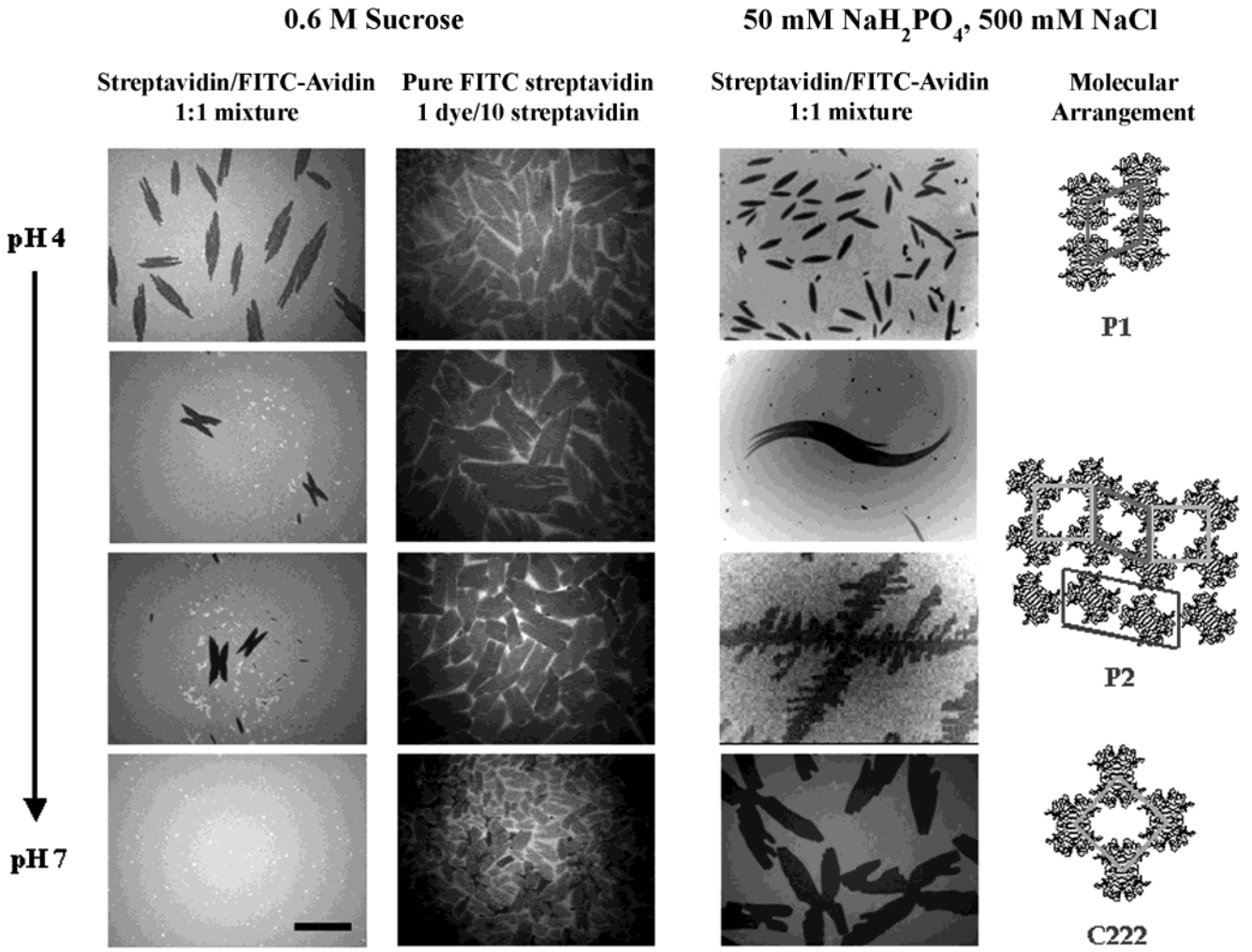

Figure 5. Fluorescence microscopic images comparing streptavidin crystal morphologies grown on lipid monolayers in either sucrose or phosphate buffer at various pH. The molecular arrangement is summarized along with the corresponding space group from Wang et al.[36] for comparison. Scale bar at bottom left is 100 μm.

presence of avidin diluted the streptavidin concentration at the surface and acted to retard nucleation and slow growth, as seen on the bilayer vesicles. Another similar trend observed among monolayer and bilayer vesicles is that fewer streptavidin crystals formed at higher pH, presumably due to the influence of the electrostatic repulsions at low ionic strengths. By adding sodium chloride to the sucrose solution at pH 7 to screen the electrostatic interactions, we were able to retrieve abundant crystals showing a square lattice with *C*222 symmetry when the streptavidin/TR avidin mixture was used. Along with the observation that fewer crystals were obtained at pH 7 with the addition of avidin, we conclude that both electrostatic interactions at high pH and the dilution of noncrystallizable avidin were responsible for impeding streptavidin crystallization.

One effect of electrostatic interactions on avidin systems has been illustrated by Velev[23] with nanometer-size biotinylated liposomes and avidin−ferritin conjugates. There they observed that, at pH 4, the avidin−ferritin molecules bound to the liposomes, but at pH 7, binding did not occur since both moieties were negatively charged. Only when positive cationic surfactant hexadecyltrimethylammonium bromide (HTAB) was mixed into the liposome to generate a more electrostatically favorable condition did avidin−ferritin conjugates begin to coat the liposomes. In our case, however, the electrostatic interactions were not strong enough to completely inhibit protein binding on the vesicles but were sufficient to obstruct crystallization.

Unlike the crystals grown in higher ionic strength buffer, analysis of lipid monolayer crystals grown in sucrose show the *C*222 space group at pH 4, 5.5, and 7. The electrostatic repulsions apparently prevent the higher density *P*1 and *P*2 crystal forms from occurring. We expect the monolayer crystals to closely resemble those on vesicle surfaces. Since the curvature of giant vesicles is negligible relative to individual streptavidin molecules, the vesicle surface is indistinguishable from that of lipid monolayers. In addition, the use of the same lipid mixtures and solution conditions produces comparable molecular interactions, and the same crystal structures, as previously confirmed with s-layer proteins.[39,45−47] The existence of one crystal structure in sucrose was consistent with the X-shaped and H-shaped morphologies seen on the surface of giant vesicles at low pH.

Conclusions

We have shown that streptavidin can be successfully crystallized on surfaces of giant biotinylated phospholipid

(45) Pum, D.; Weinhandl, M.; Hödl, C.; Sleytr, U. B. *J. Bacteriol.* **1993**, *175*, 2762−2766.
(46) Wetzer, B.; Pfandler, A.; Györvary, E.; Pum, D.; Lösche, M.; Sleytr, U. B. *Langmuir* **1998**, *14*, 6899−6906.
(47) Pum, D.; Sára, M.; Sleytr, U. B. *J. Bacteriol.* **1989**, *171*, 2596−5303.

vesicles in sucrose solution. The crystal-coated vesicles took on either a spherical or prolate ellipsoidal appearance with a narrow aspect ratio distribution. By performing laser scanning confocal microscopy on the crystal-coated vesicles, we found that roughened spheres and ellipsoids formed via different mechanisms. Roughened spheres carry smaller, randomly oriented crystalline patches on the vesicle surface, whereas ellipsoids tend to have larger, continuous crystallites with fewer grain boundaries and defects. Confocal microscopy also allowed us to observe various crystal morphologies on vesicle surfaces under different solution conditions. The number and size of crystal domains can be roughly controlled by the addition of noncrystallizable avidin and by controlling the solution pH. The crystal morphologies do not follow the trend normally seen with those grown on lipid monolayers in ionic buffer solutions at various pH values. Due to the lack of ionic species in sucrose solution, the electrostatic repulsion prevented other higher density crystal structures from forming, and only the lowest density *C*222 symmetry was observed.

Acknowledgment. We thank Roger Kornberg for allowing us the use of his image processing facilities. This work was supported by NASA Grant NAG3-2398 and Grant Me1458/3 by the Deutsche Forschungsgemeinschaft (DFG).

LA025568V